

Rectified Momentum Transport for a Kicked Bose-Einstein Condensate

Mark Sadgrove,^{1,2,*} Munekazu Horikoshi,³ Tetsuo Sekimura,¹ and Ken'ichi Nakagawa^{1,2}

¹*Institute for Laser Science, The University of Electro Communications, Chofushi, Chofugaoka 1-5-1, Japan*

²*Japan Science and Technology Agency, Kawaguchi, Saitama, 332-0012, Japan*

³*The University of Tokyo, 2-11-16 Yayoi, Bunkyo-ku, Tokyo 113-8656, Japan.*

(Received 16 March 2007; published 25 July 2007)

We report the experimental observation of rectified momentum transport for a Bose-Einstein condensate kicked at the Talbot time (quantum resonance) by an optical standing wave. Atoms are initially prepared in a superposition of the 0 and $-2\hbar k_l$ momentum states using an optical $\pi/2$ pulse. By changing the relative phase of the superposed states, a momentum current in either direction along the standing wave may be produced. We offer an interpretation based on matter-wave interference, showing that the observed effect is uniquely quantum.

DOI: [10.1103/PhysRevLett.99.043002](https://doi.org/10.1103/PhysRevLett.99.043002)

PACS numbers: 32.80.Qk, 03.75.-b, 05.45.Mt

The current interest in rectified atomic diffusion, or atomic ratchets, may be traced back to fundamental thermodynamical concerns [1] and also the desire to understand the so-called ‘‘Brownian motors’’ linked to directed diffusion on a molecular scale [2,3]. Abstractly, the ratchet effect may be defined as the inducement of directed diffusion in a system subject to unbiased perturbations due to a broken spatiotemporal symmetry.

Given the scale on which such microscopic ratchets must work, it is not surprising that the concept of *quantum ratchets* has recently augmented this area of investigation. The addition of quantum effects such as tunneling gives rise to new ratchet phenomena such as current reversal [4]. Whilst early quantum ratchet investigations, both theoretical and experimental, have focused on the role of dissipative fluctuations in driving a ratchet current [5], recent theory has considered the possibility of *Hamiltonian ratchets*, where the diffusion arises from Hamiltonian chaos rather than stochastic fluctuations [6]. This has led to proposals [7,8] and even an experimental realization [9] for ratchet systems realized using atom optics, in the context of the *atom optics kicked rotor* [10] where periodic pulses from an optical standing wave kick atoms into different momentum states.

It is generally accepted that a ratchet effect cannot be produced without breaking the spatiotemporal symmetry of the kicked rotor system. In Ref. [9], a rocking sine wave potential was combined with broken time symmetry of the kicking pulses to effectively realize such a system in an experiment. Other schemes involve the use of quantum resonance (QR) to drive the ratchet effect. At QR, atoms typically exhibit linear momentum growth *symmetrical* about the initial mean momentum. However, it has been suggested that merely breaking the spatial symmetry of the kicked rotor at QR may be sufficient to produce a ratchet current [11]. In this Letter we present the first experimental evidence of such a resonant ratchet effect in which the

underlying mechanism is *purely quantum*. Our system uses a Bose-Einstein condensate (BEC) kicked by an optical standing wave [12], but there is no asymmetry in either the kicking potential or the period of the kicks (which is set to the Talbot time T_T corresponding to quantum resonance [13]). Rather, the observed directed diffusion is a property of the initial atomic wave function (which we prepare before kicking) in the presence of a resonantly pulsed optical lattice. The experiment *cannot* be performed with thermal atoms, as it requires an initial atomic momentum spread much less than a photon recoil in order to avoid dephasing effects. Our work presents analytical, simulation, and experimental results for a specific realization of a ratchet at QR similar to that proposed in [11]. We also offer a clear physical interpretation in terms of matter-wave interference.

As shown in Fig. 1, our experiment is comprised of a BEC which is subjected to pulses from an optical standing wave. The experimental configuration has been explained elsewhere [14,15] and thus we provide only a summary here. A BEC of $\sim 3 \times 10^3$ ^{87}Rb atoms is realized and loaded onto an atom chip [15]. The atoms are trapped in the $5S_{1/2}$, $F = 2$, $m_f = 2$ state by the magnetic field generated by the chip and sit $700 \mu\text{m}$ below the chip surface. Typically, the axial trapping frequency for the BEC is $\omega_z \approx 2\pi \times 17 \text{ Hz}$ and the axial and radial Thomas-Fermi radii are $d_z = 17 \mu\text{m}$ and $d_\rho = 3 \mu\text{m}$, respectively. The BEC is prepared in an initial superposition state using a Bragg $\pi/2$ pulse and then kicked using light from a diode laser. Figure 1(a) shows the configuration used to control the intensity and frequency of the two beams used to create the Bragg and kicking pulses. A free running 100 mW diode laser, red detuned 4 GHz (i.e., $\lambda = 780.233 \text{ nm}$) from the ^{87}Rb $5^2S_{1/2} \rightarrow 5^2P_{3/2}$ transition, enters a 50/50 beam splitter and the output beams are passed through separate acousto-optic modulators (AOMs) to control their frequency and amplitude after which they intersect with

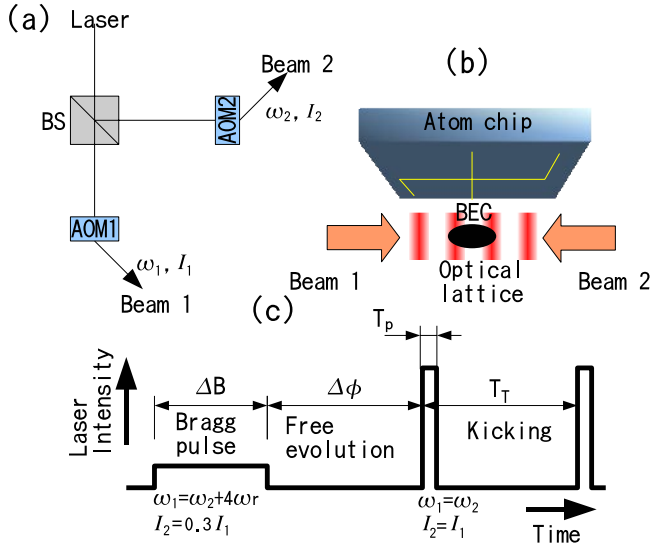


FIG. 1 (color online). Diagrams of the experimental setup and sequence. In (a), the laser configuration used to control Bragg diffraction and the kicking beam is shown. The beam is split by a 50/50 beam splitter (BS) and the output light passes through separate acousto-optic modulators (AOM) which control the beam intensities $I_{1,2}$ and frequencies $\omega_{1,2}$. The atom chip BEC setup is shown schematically in (b) along with the optical lattice created by the two intersecting beams. The three different phases of Bragg diffraction, phase evolution, and kicking are shown in (c) and are explained further in the text.

the BEC [Fig. 1(b)]. The experimental sequence of laser pulses is shown in the diagram in Fig. 1(c).

For the Bragg pulse, the intensity of one beam is dropped to 3% of its maximum power using the amplitude modulation (AM) mode of one function generator while the frequency of the counterpropagating beam is increased by $4\omega_r \approx 15$ kHz (where $\omega_r = 2.37 \times 10^4$ Hz is the recoil frequency of ^{87}Rb) relative to the other beam. After the Bragg pulse, a period Δ_ϕ of free evolution is used to adjust the quantum phase of the $|-2\hbar k_i\rangle$ state relative to $|0\hbar k_i\rangle$, and the beam intensity and frequencies are made equal for kicking. The overall pulse envelope and timing were controlled by another pulse generator. The Bragg or kicking beams have an optical power of about 5 mW. For a $\pi/2$ pulse, a duration Δ_B of $60 \mu\text{s}$ was used. For the kicking pulses, a width of $T_p = 5 \mu\text{s}$ was used with a pulse period T equal to the Talbot time $T_T = \pi/2\omega_r \approx 66.3 \mu\text{s}$ for ^{87}Rb . Like other groups performing kicked BEC experiments [12], we have found that neither the energy due to atom-atom interactions nor the harmonic potential affects our results for the time scales used here, given the relatively much greater energy due to kicking of the atoms. We simulate the system by calculating the evolution of the initial wave function subject to the single atom Hamiltonian \hat{H} (i.e., simulation of the Gross-Pitaevskii equation is not necessary).

We now provide a theoretical treatment of our system. First we consider the preparation of the initial state by a

Bragg $\pi/2$ pulse. We will assume the BEC starts in an initial 0 momentum eigenstate $|0\hbar k_i\rangle$. This is not a bad approximation, since the atoms in the BEC have a thermal spread which is much less than $2\hbar k_i$. The $\pi/2$ pulse creates an equally weighted superposition state $|\psi_B\rangle = \frac{1}{\sqrt{2}} \times (|0\hbar k_i\rangle - i|2\hbar k_i\rangle)$. After the Bragg pulse has been applied, a period Δ_ϕ of free evolution is allowed. During this time, the $|-2\hbar k_i\rangle$ state accumulates a phase $\phi = 4\omega_r \Delta_\phi$, where $\phi = 2\pi$ corresponds to $\Delta_\phi = T_T$. The initial state just before kicking starts is then

$$|\psi_i\rangle = \frac{1}{\sqrt{2}} (|0\hbar k_i\rangle - ie^{i\phi} |-2\hbar k_i\rangle). \quad (1)$$

The dynamics, due to sharp periodic momentum kicks applied to this state, are governed by the Hamiltonian [16]

$$\hat{H} = \frac{\hat{p}^2}{2} + K \cos(2k_i \hat{x}) \sum_t \delta(t' - t\tau), \quad (2)$$

where \hat{p} and \hat{x} are the atomic momentum and position operators, respectively, $K = \hbar V_0 T_p / \hbar$ is the kicking strength for an optical potential of height V_0 , t' is time, t is the kick counter, and $\tau = 4\pi T / T_T$ is the scaled kicking time. The associated Floquet operator for the case of QR ($\tau = 4\pi$) is [17] $\hat{U}_{\text{QR}}(t) = \exp[-iKt \cos(2k_i \hat{x})]$. Applied to $|\psi_i\rangle$, the output wave function ψ_o and momentum distribution $P(m)$ are [18]

$$\psi_o(m) = \frac{e^{-i\tau m}}{\sqrt{2}} [J_m(Kt) - e^{i\phi} J_{m+1}(Kt)], \quad (3)$$

$$P(m) = \frac{1}{2} [J_m^2(Kt) + J_{m+1}^2(Kt) - 2 \cos \phi J_m(Kt) J_{m+1}(Kt)]. \quad (4)$$

Equations (3) and (4) have a particularly interesting property: for general phase ϕ , the wave function and thus the momentum distribution *grow asymmetrically with time*. This property is seen in Figs. 2(a) and 2(b) which show the wave function after 5 kicks for $\phi = \pi$. The change in net momentum may be seen to be due to interference between the diffraction orders of the two initial wave functions which is mostly destructive below $m = -1$ but constructive above this initial mean momentum, leading to an asymmetric distribution of atoms [Fig. 2(c)]. The dramatic nature of this induced asymmetry is demonstrated even more clearly in [Fig. 2(d)] which shows the theoretical probability distribution after 100 kicks. We note that the directed transport of atoms has been caused by the interference of diffracted matter waves, that is, the observed “ratchet” effect is *entirely quantum* (indeed, our experiment may be viewed as a type of atom interferometer [19]). Experimental confirmation is presented in Fig. 3 which shows absorption images of a kicked BEC after

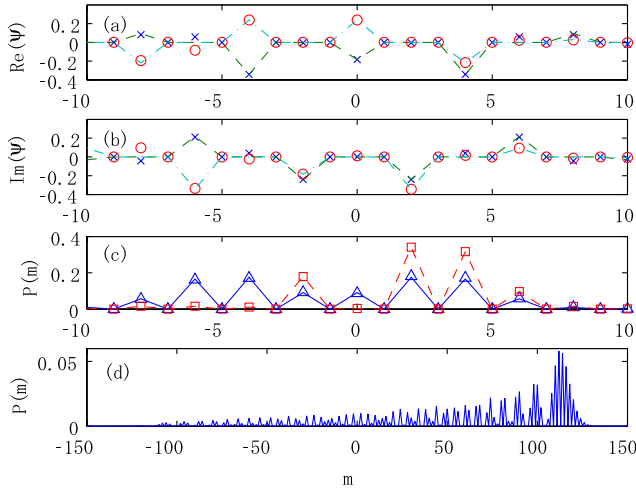


FIG. 2 (color online). Wave functions and momentum probability distributions for kicked atoms with $K = 0.6$. The momentum m is in units of $2\hbar k_l$. In (a) and (b), respectively, the real and imaginary parts of atomic wave functions after 5 kicks for $\phi = \pi$ are shown. The wave function evolving from an initial $|0\hbar k_l\rangle$ state is shown with x 's (simulations) and a dot-dashed line [theory of Eq. (3)], while that which evolved from an initial $|-2\hbar k_l\rangle$ state is shown with \circ 's (simulations) and a dotted line (theory). The lines are merely to guide the eye, and the theoretical wave function is only nonzero at multiples of $m = 2\hbar k_l$. In (c) asymmetry is seen to arise in the final momentum probability distribution corresponding to $\phi = \pi$ (dashed line—theory, squares—simulations) while for $\phi = \pi/2$ (solid line—theory, triangles—simulations) there is symmetry about $m = -\hbar k_l$. In (d) the same system is shown after 100 kicks emphasizing the extreme asymmetry of the momentum distribution.

preparation into state ψ_i . The behavior seen matches that predicted by Eq. (4). In particular, for $\phi = 0$ the atomic momentum distribution increases in asymmetry towards negative momentum, whereas for $\phi = \pi$, the asymmetry is in the opposite direction. For $\phi = \pi/2$ the distribution is almost symmetrical (allowing for experimental fluctuations).

We may also find the momentum current $i(t) = (d/dt) \times \langle p(t) \rangle$ by calculating the first moment of the momentum distribution $\langle p \rangle = \sum_m m P(m) = \frac{1}{2} \sum_m [m J_m^2(Kt) + m J_{m+1}^2(Kt) - 2 \cos(\phi) m J_m(Kt) J_{m+1}(Kt)]$. The first two terms give the momenta of the two superposed initial states, e.g., 0 and -1 (in $2\hbar k_l$ units), respectively. The term of interest is $\sum_m m J_m(Kt) J_{m+1}(Kt)$, which may be summed by applying the standard Bessel recursion formula and the Neuman sum rule [20] to give $Kt/2$. Thus

$$i(t) = \frac{d}{dt} \langle p(t) \rangle = -\cos\phi \frac{K}{2}. \quad (5)$$

Equation (5) offers a useful way to summarize the data. The atomic momentum distribution was reconstructed from the absorption images shown in Fig. 3 and the

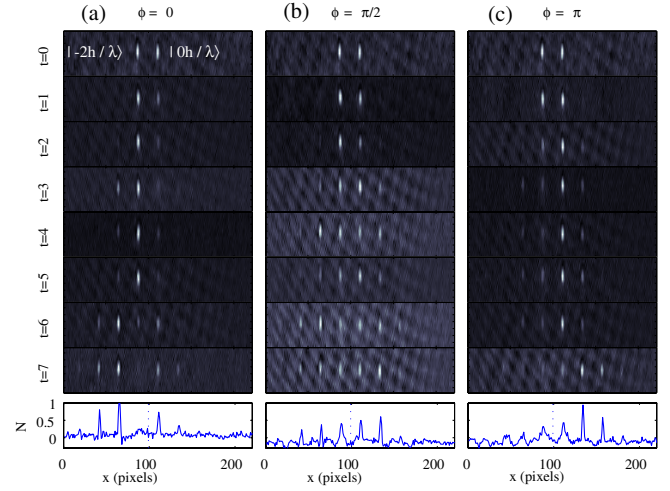


FIG. 3 (color online). Sequences of absorption images for the ratchet BEC experiment from $t = 0$ to $t = 7$ kicks for (a) $\phi = 0$, (b) $\phi = \pi/2$, and (c) $\phi = \pi$. The $t = 0$ case shows the initial distribution after the Bragg $\pi/2$ pulse. In the top panel of (a), the 0 and $-2\hbar k$ momentum states are shown. At the bottom of each column, a sum over the rows of the image for $t = 7$ is shown giving the distribution of atom number N with position. In these plots, the dashed line marks the position of the mean initial momentum $\hbar k$. The images clearly show the presence of a ratchet current which reverses direction when the phase ϕ crosses $\pi = \phi/2$ (for which phase the current is seen to vanish).

mean momentum calculated. To check repeatability we took another set of data for the same parameters as those in Fig. 3, for $t > 2$ (since very little diffusion occurs in the first two kicks). Average currents for the two data sets are shown in Fig. 4, along with error bars showing the difference between the measurements. The extraction of very small mean momenta ($\langle p \rangle \sim \hbar k_l$) from the distributions in Fig. 3 is hampered by experimental imperfections such as CCD noise and scattered light, and laser frequency drift, which may lead to occasional changes in experimental parameters. This is the most likely cause of the large error bar seen in the case of $\phi = \pi$ when $t = 6$. Increasing the accuracy of the measurements would require a larger atom number and ideally a separate laser for Bragg diffraction and kicking. Nonetheless, Fig. 4 clearly demonstrates the momentum current effect and a current reversal for $\phi = 0$ compared with $\phi = \pi$. The data show a general linear trend as predicted by Eq. (5), with fitted lines shown in both cases. For $\phi = \pi/2$, although individual momentum distributions are not perfectly symmetrical, the current is near 0 on average. The control case for an initial $|0\hbar k_l\rangle$ distribution is also shown and seen to exhibit near 0 average momentum current. Note that the dotted and dashed lines are not fits to the data, since there are no free parameters in either of these cases. Theoretically, the momentum current should persist indefinitely. In an experimental setting, however, imperfections such as the finite pulse width and any small difference between the pulse period and the Talbot time will reduce the ratchet

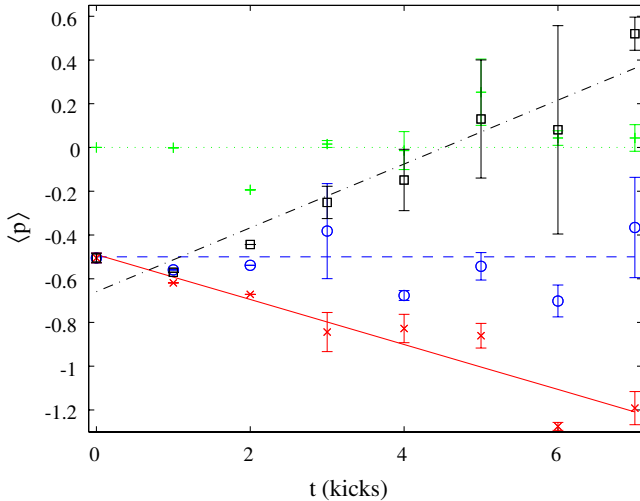


FIG. 4 (color online). The experimentally measured $\langle p \rangle$ (in units of $2\hbar k_l$) is shown along with theoretical curves for various initial conditions. Experimental data are shown by x ($\phi = 0$), \circ ($\phi = \pi/2$), \square ($\phi = \pi$), and $+$ (no initial $\pi/2$ pulse). The solid and dash-dotted lines are fits to the data for $\phi = 0$ and $\phi = \pi$, respectively. Dashed and dotted lines show $\langle p \rangle = -0.5$ and $\langle p \rangle = 0$, respectively (note that these lines are not fits to the data).

current. Because of a low signal to noise ratio at higher kick numbers in the current experiment, it was not possible to probe these effects with our current setup. We note that the effects seen here require a well-defined quantum phase between the initial states in superposition. Therefore, the experiment must be performed using a BEC as a thermal cloud typically has a large spread of initial momenta (and therefore quantum phase after free evolution), destroying the directed diffusion effect. It may be possible to exploit any sensitivity of the ratchet current to pulse timing and phase variations to make accurate interferometry measurements.

In summary, we have demonstrated a novel quantum ratchet effect, in which directed momentum transport occurs in a system subject to a pulsed potential with no net bias. The effect has no classical analogue, unlike previous such systems studied experimentally. The direction of the ratchet current varied with the initial quantum phase as predicted, showing complete reversal for $\phi = 0$ compared with $\phi = \pi$. This realization of directed momentum transport suggests new possible mechanisms for directed motion on any scale where quantum interference effects are non-negligible and resonant transport exists.

M.S. would like to thank Scott Parkins and Andrew Daley for discussions regarding this work.

Note added in proof.—After submission of this Letter, similar experimental results were reported by Dana *et al.* [21].

*mark@ils.uec.ac.jp

- [1] R. P. Feynman, *The Feynman Lectures on Physics* (Addison-Wesley, Reading, MA, 1963), Vol. 1, Chap. 46.
- [2] R. D. Astumian and P. Hänggi, *Phys. Today* **55**, No. 11, 33 (2002).
- [3] P. Riemann, *Phys. Rep.* **361**, 57 (2002).
- [4] P. Riemann, M. Grifoni, and P. Hänggi, *Phys. Rev. Lett.* **79**, 10 (1997).
- [5] M. Schiavoni *et al.*, *Phys. Rev. Lett.* **90**, 094101 (2003); G. C. Carlo *et al.*, *ibid.* **94**, 164101 (2005); S. Flach, O. Yevtushenko, and Y. Zolotaryuk, *ibid.* **84**, 2358 (2000).
- [6] H. Schanz *et al.*, *Phys. Rev. Lett.* **87**, 070601 (2001); J. Gong and P. Brumer, *Phys. Rev. Lett.* **97**, 240602 (2006).
- [7] C. Mennerat-Robilliard *et al.*, *Phys. Rev. Lett.* **82**, 851 (1999); T. S. Monteiro *et al.*, *Phys. Rev. Lett.* **89**, 194102 (2002).
- [8] G. C. Carlo *et al.*, *Phys. Rev. A* **74**, 033617 (2006); D. Poletti *et al.*, arXiv:cond-mat/0609535.
- [9] P. H. Jones *et al.*, *Phys. Rev. Lett.* **98**, 073002 (2007).
- [10] F. L. Moore *et al.*, *Phys. Rev. Lett.* **75**, 4598 (1995).
- [11] E. Lundh and M. Wallin, *Phys. Rev. Lett.* **94**, 110603 (2005); D. Poletti, G. C. Carlo, and B. Li, *Phys. Rev. E* **75**, 011102 (2007); S. Denisov, L. Morales-Molina, and S. Flach, arXiv:cond-mat/0607558.
- [12] G. J. Duffy *et al.*, *Phys. Rev. A* **70**, 041602(R) (2004); S. Wimberger *et al.*, *Phys. Rev. Lett.* **94**, 130404 (2005); G. Behinaein *et al.*, *Phys. Rev. Lett.* **97**, 244101 (2006).
- [13] C. Ryu *et al.*, *Phys. Rev. Lett.* **96**, 160403 (2006).
- [14] M. Horikoshi and K. Nakagawa, *Phys. Rev. A* **74**, 031602(R) (2006).
- [15] M. Horikoshi and K. Nakagawa, *Appl. Phys. B* **82**, 363 (2006).
- [16] R. Graham, M. Schlautmann, and P. Zoller, *Phys. Rev. A* **45**, R19 (1992).
- [17] F. M. Izrailev and D. L. Shepelyansky, *Sov. Phys. Dokl.* **24**, 996 (1979) [*Theor. Math. Phys. (Engl. Transl.)* **43**, 553 (1980)].
- [18] D. Cohen, *Phys. Rev. A* **44**, 2292 (1991).
- [19] M. R. Andrews *et al.*, *Science* **275**, 637 (1997).
- [20] G. N. Watson, *A Treatise on the Theory of Bessel Functions* (Cambridge University Press, Cambridge, England, 1996).
- [21] I. Dana, V. Ramareddy, I. Talukdar, and G. S. Summy, arXiv:0706.0871v1.